Chapter 4

Improvement of Field Emission Characteristics through the Structures of Intermixture of Long and Short Carbon Nanotubes

Density control of carbon nanotubes is one of the most effective ways to improve the field emission characteristics. Unlike previous studies which always reduce the numbers of CNTs to achieve the object of density control, a novel density control with the structure of intermixture of long and short carbon nanotubes is first synthesized. Appropriately choosing the pre-treatment times and the contents of hydrogen can achieve this novel density control of CNTs. Atomic force microscopy (AFM) and scanning electron microscopy (SEM) are used to examine the morphology of catalytic nanoparticles and carbon nanotubes. The turn-on fields decrease from 3.4 to 2.2V/μm and the field emission current density increases from 21 to 400mA/cm^2 at 6.46V/μm when the pre-treatment times decrease from 10min to 5min. The turn-on fields decrease from 4.4 V/μm to 2.2 V/μm and the field emission current density increases from 0.045mA/cm^2 to 400mA/cm^2 at 6.46V/μm when the contents of hydrogen increase from 10% to 50%. Besides, the best threshold field is about 3.64 V/μm with 5 min pre-treatment of 50% hydrogen content. Therefore, we have successfully demonstrated that this novel density control of CNTs can greatly

improve the field emission characteristics.

4.1 Introduction

Since the first discovery of CNTs by Iijima in 1991[4.1], carbon nanotubes (CNTs) have attracted a great deal of intense academic and commercial interest due to their remarkable properties and their many potential applications, for example, in cold cathodes for field–emission displays [4.2], tips for scanning probe microscopes or biological probes [4.3], sensors [4.4], and quantum wires for nanoscale electronics [4.5-4.6]. In particular, CNTs have become one of the most promising candidates for field emission electron source and various vacuum microelectronic devices by the properties such as their high aspect ratio, high mechanical strength, chemical stability, super thermal conductivity, extremely low applied threshold field, and easily deliver a relatively high emission current density [4.7-4.8].

Efforts have been made to improve the field emission properties of carbon nanotubes, including purification [4.9] and doping [4.10], but it has been reported that the most effective ways are the density control of CNTs. For high density CNTs, screening effect reduces the field enhancement and thus reduces emitted current. For low density CNTs, the current density decreases due to the decreasing emission sites. Therefore the density control of CNTs plays a significant role in the field emission

properties, and theoretical value of the optimal CNTs' density was calculated as 2.5 x 10^7emitters/cm^2. There are several methods to control the density of CNTs like different aspect ratios of anodic aluminium oxide (AAO) nanochannels [4.11], NH_3 plasma treatment of catalyst film [4.12], pulse-current electrochemical deposition [4.13], and plasma post treatment on CNTs film. However, the density of CNTs is still very high and cannot be controlled effectively. In this study, we propose a new type of density control of CNTs with the structures of intermixture of long and short carbon nanotubes by appropriately choosing the pre-treatment time and the contents of hydrogen. Obviously, the density of each of long and short sets of CNTs will be reduced effectively because the numbers of CNTs have been divided into two sets. Until now, this novel density control of CNTs composed of two sets of different lengths has not been reported.

4.2 **Effects of Different Pre-treatment Times**

4.2.1 Experimental Procedures

In this study, the fabrication procedures of CNTs are listed as below. A 1 μm-thick photoresist is spin-coated on an n-type Si (100) substrate and square cells with an emission area $25x10^{-4}$ cm^2 are patterned by photolithography. Then a Ti layer of 50nm and a thin Fe (~5 nm) catalytic layer are subsequently deposited on the photoresist patterned Si substrate by electron beam evaporation system. Afterward,

the patterned film is formed after the photoresist is removed by the lift-off method. Finally, CNTs a grown selectively on the iron layers by the atmospheric pressure thermal chemical vapor deposition.

The thermal CVD reactor is a 2-in.-diameter horizontal quartz tube furnace. Samples are placed horizontal up into the reactor at about 400°C, and then be heated to 700°C at 100°C/min in pure N_2 with the flow rate at 1000 sccm. When the temperature is stabilized, pure N_2 gas will be kept flowing for about 8 min. Here, we call this process as annealing process. After finishing annealing process, N_2/H_2 mixture gases are fed into the furnace to pre-treat the catalytic film with the same gas flow rate at 500sccm. The pre-treatment times are 5 and 10 min, respectively. Finally, C_2H_4 at 20 sccm is added to the N_2/H_2 mixture gases for CNTs' growth. The gas pressure is held at about 1 atm and the growth time is 10 min. Atomic force microscopy (AFM) and scanning electron microscopy (SEM) are used to examine the morphology of catalytic nanoparticles and carbon nanotubes. The field emission tests are measured in a parallel plate diode configuration at room temperature in vacuum of ~ 5×10^{-6} Torr. The spacer between the anode and CNTs cathode is approximately 120 μm and the emitting area is 25×10^{-4} cm^2. The field emission current is measured as a function of the anode voltage.

4.2.2 Results and Discussion

Figures 4-1(a)-4-1(c) show the AFM images of the surface morphology of the catalyst film under different pre-treatment time. The scan size of each image is 5 x 5 μm^2. Figure 4-1(a) shows AFM image of iron film after 700°C annealing in pure N_2. The image reveals that iron film do not break into nanoparticles well, but with small iron nanoparticles and larger iron nanoparticles still agglomerate. The surface roughness is very high and the root mean square of the surface roughness is approximately 14.146nm. Figure 4-1(b) and 4-1(c) show AFM images of iron film to be pre-treated in N_2/H_2 mixture gases at 700°C for 5 min and 10 min, respectively. The root mean squares of the surface roughness are 8.096nm and 7.211nm, respectively. It is observed that the density of nanoparticles increases and the number of larger nanoparticles decreases when the pre-treatment time increases to 10 min. The surface roughness of the iron film after 10 min pre-treatment become smooth and the size of nanoparticles are somewhat uniform in several tens of nanometer except some nanoparticles are still larger. Figures 4-2(a)-4-2(c) show the SEM images of the catalyst film after different pre-treatment times. Figure 4-2(a) shows that iron film just starts to break into nanoparticles after annealing process. Most of the nanoparticles still agglomerate together and the larger ones seem to lie on the top of the small agglomerated iron nanoparticles. Figure 4-2(b) shows that iron film is pre-treated at 700°C in N_2/H_2 mixture gases for 5 min. The size distribution of most of the iron

nanoparticles is in the range of several tens of nanometer but with a lot of larger nanoparticles exceeding one hundred nanometers. Figure 4-2(c) shows that iron film is pre-treated at 700°C in N_2/H_2 mixture gases for 10 min. The size distribution of most of the iron nanoparticles is in the range of several tens of nanometer except fewer larger nanoparticles exceeding one hundred nanometers.

Figure 4-3 shows the SEM images of CNTs under different pre-treatment times. It is observed that the CNTs produced are spilt into two sets being composed of the structures of intermixture of long and short carbon nanotubes in the 5 min pre-treatment case. One set is about 2 times longer than the other and some of the longer CNTs are with larger diameter. Figures 4-2(a) and 4-2(c) show the SEM image of CNTs grown under 0 min and 10 min pre-treatment, respectively. It is observed that the density of longer nanotubes protruding out of the lower set of CNTs decreases. The phenomena of the two sets of CNTs become less obvious, as shown in figs 4-2(a) and 4-2(c).

However, the reason that some CNTs grow faster than the others is still not clear. We propose the possible explanation as follows. The longer carbon nanotubes probably grow from the larger nanoparticles [4.14]. When we examine AFM images of figure 4-1(c) or SEM images of figure 4-2(c), small iron nanoparticles can be seen covering the areas between the countable larger nanoparticles in the case of 10 min

pre-treatment. It is observed that longer and wider nanotubes protrude among the shorter nanotubes are relatively few. In the case of 5 min pre-treatment, the numbers of larger nanoparticles increase and a lot of longer nanotubes grow as can be seen in figure 4-3 (b). Therefore, we indirectly explain this phenomenon of the growth of two sets of CNTs. Anyway, the two sets of CNTs really provide a novel density control of carbon nanotubes. The separation between CNTs of each of the two sets is greater than that is typically observed in the growth of CNTs. Therefore, the corresponding density of each set of CNTs is reduced and this novel morphology of CNTs will be subject to less field screening from surrounding nanotubes [4.15].

Figure 4-4(a) shows the field-emission properties of CNTs with different pre-treatment times. The corresponding Fowler-Nordheim plots are shown in Fig. 4-4(b) and the linearity of the F-N plot confirmed the field-emission phenomenon. When the pre-treatment times decrease from 10 to 5min, the turn-on fields decrease from 3.4 to 2.2V/μm and the field emission current density increases from 21mA/cm^2 to 400mA/cm^2 at 6.46V/μm. The threshold fields are about 6.66, 3.64 and 5.36 V/μm for 0, 5 and 10 min pre-treatment, respectively.

4.3 Effects of H_2 Flow Rate during Pre-treatment

4.3.1 Experimental Procedures

In this study, the fabrication procedures of CNTs are listed as below. A 1

μm-thick photoresist is spin-coated on an n-type Si (100) substrate and square cells with an emission area $25x10^{-4}$ cm^2 are patterned by photolithography. Then a Ti layer of 50nm and a thin Fe (~5 nm) catalytic layer are subsequently deposited on the photoresist patterned Si substrate by electron beam evaporation system. Afterward, the patterned film is formed after the photoresist is removed by the lift-off method. Finally, CNTs are grown selectively on the iron layers by the atmospheric pressure thermal chemical vapor deposition.

Samples are placed horizontal up into the reactor at about 400°C, and then be heated to 700°C at 100°C/min in pure N_2 with the flow rate at 1000 sccm. When the temperature is stabilized, pure N_2 gas will be kept flowing for about 8 min. Here, we call this process as annealing process. After finishing annealing process, N_2/H_2 mixture gases are fed into the furnace to pre-treat the catalytic film with total flow rate fixed at 1000sccm. The pre-treatment time is 5min and the contents of hydrogen are 10%, 30% and 50% of N_2/H_2 mixture gases, respectively. Finally, C_2H_4 at 20 sccm is added to the N_2/H_2 mixture gases (500sccm/500sccm) for CNTs' growth. The gas pressure is held at about 1 atm and the growth time is 10 min. Scanning electron microscopy (SEM) are used to examine the morphology of catalytic nanoparticles and carbon nanotubes. The field emission tests are measured in a parallel plate diode configuration at room temperature in vacuum of ~ 5×10^{-6} Torr. The spacer between

the anode and CNTs cathode is approximately 120 μm and the emitting area is $25x10^{-4}$ cm^2. The field emission current is measured as a function of the anode voltage.

4.3.2 Results and Discussion

Figures 4-5-4-7 show SEM images of CNTs grown under different hydrogen contents during pre-treatment. It is observed that the density of CNTs is increased when the content of hydrogen increases. Besides, the phenomena of the structures of intermixture of long and short carbon nanotubes become obvious when the content of hydrogen increases. As discussed above, the separation between CNTs with the structure of intermixture of long and short nanotubes is increased when the content of hydrogen increase. Therefore, the corresponding density of each set of CNTs is reduced and this novel morphology of CNTs will be subject to less field screening from surrounding nanotubes [4.15].Besides, the total field emission sites will not be reduced when compares to previous methods of density control.

Figure 4-8(a) shows the field-emission properties of CNTs with different contents of hydrogen. The corresponding Fowler-Nordheim plots are shown in Fig. 4-8(b) and the linearity of the F-N plot confirmed the field-emission phenomenon. The turn-on fields decrease from 4.4 V/μm to 2.2 V/μm and the field emission current density increases from 0.045mA/cm^2 to 400mA/cm^2 at 6.46V/μm when the contents

of hydrogen increase from 10% to 50%. The threshold fields are about 5.5 and 3.64 V/μm for 30% and 50% hydrogen contents, respectively.

4.4 Conclusions

Due to the sparse nanotubes and relatively short distance between nanotube and anode, the set of longer CNTs will emit electrons earlier than the shorter set of CNTs. Therefore, the field screening effect is reduced and the turn-on field can be decreased. When the applied electric field increases to certain value, not only the longer set of CNTs emit electrons, but also the shorter set of CNTs will start to emit electrons. Finally, the field emission current density will increase very fast in a short range of electric field.

In conclusion, this novel density control of carbon nanotubes not only reduces the density of CNTs but also keeps the field emission sites not to be reduced. Lower turn-on field and ultra high field emission current density can be achieved. When the pre-treatment times decrease from 10 to 5min, the turn-on fields decrease from 3.4 to 2.2V/μm and the field emission current density increases from 21 to 400mA/cm^2 at 6.46V/μm. The turn-on fields decrease from 4.4 V/μm to 2.2 V/μm and the field emission current density increases from 0.045mA/cm^2 to 400mA/cm^2 at 6.46V/μm when the contents of hydrogen increase from 10% to 50%. Besides, the best threshold field is about 3.64 V/μm with 5 min pre-treatment of 50% hydrogen content.

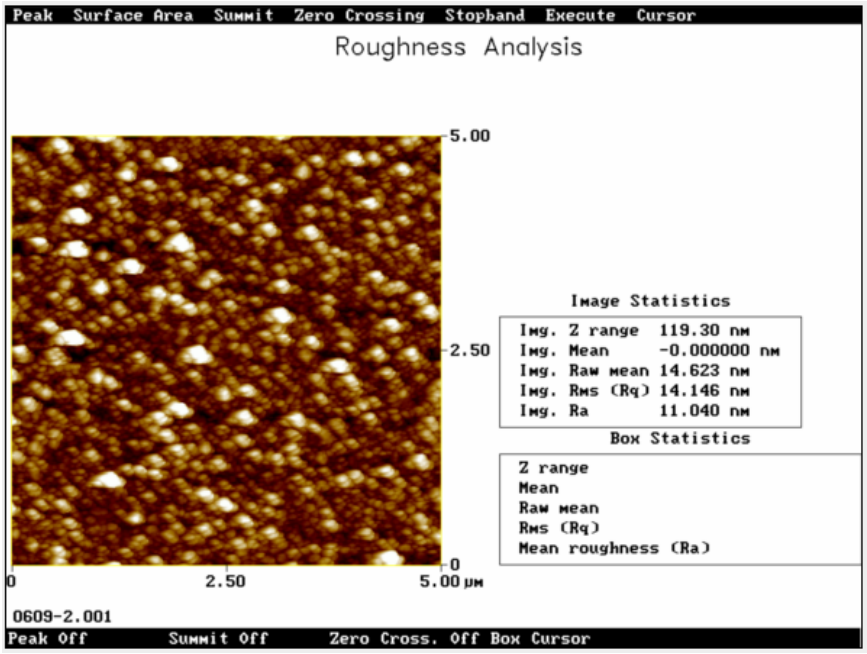
Peak Surface Area Summit Zero Crossing Stopband Execute Cursor
Roughness Analysis
5.00
2.50
0
0
2.50
5.00 µm
Image Statistics
Img. Z range 119.30 nm
Img. Mean -0.000000 nm
Img. Raw mean 14.623 nm
Img. Rms (Rq) 14.146 nm
Img. Ra 11.040 nm
Box Statistics
Z range
Mean
Raw mean
Rms (Rq)
Mean roughness (Ra)
0609-2.001
Peak Off Summit Off Zero Cross. Off Box Cursor

(a)

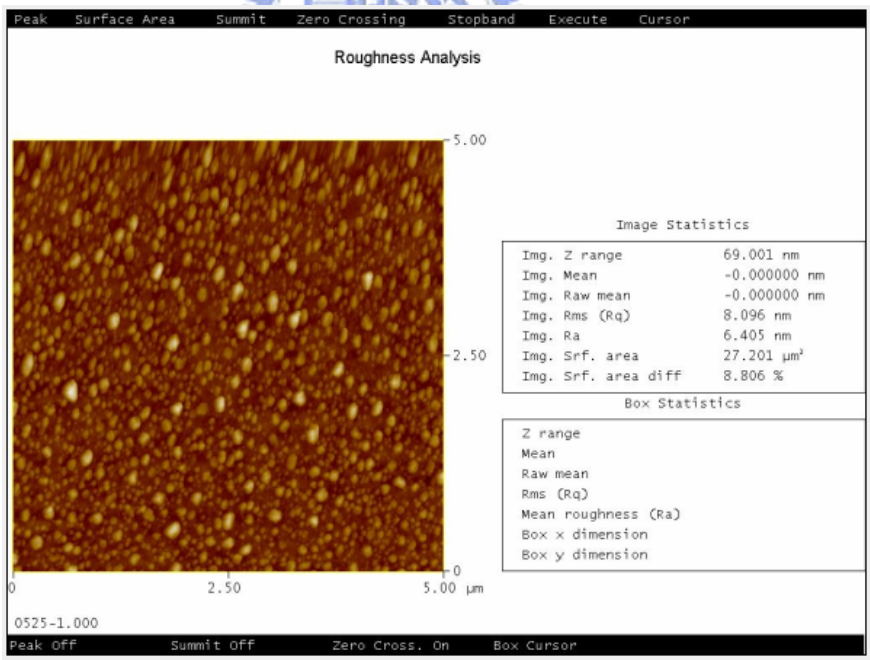
Peak Surface Area Summit Zero Crossing Stopband Execute Cursor
Roughness Analysis
5.00
2.50
0
0
2.50
5.00 µm
Image Statistics
Img. Z range 69.001 nm
Img. Mean -0.000000 nm
Img. Raw mean -0.000000 nm
Img. Rms (Rq) 8.096 nm
Img. Ra 6.405 nm
Img. Srf. area 27.201 µm²
Img. Srf. area diff 8.806 %
Box Statistics
Z range
Mean
Raw mean
Rms (Rq)
Mean roughness (Ra)
Box x dimension
Box y dimension
0525-1.000
Peak Off Summit Off Zero Cross. On Box Cursor

(b)

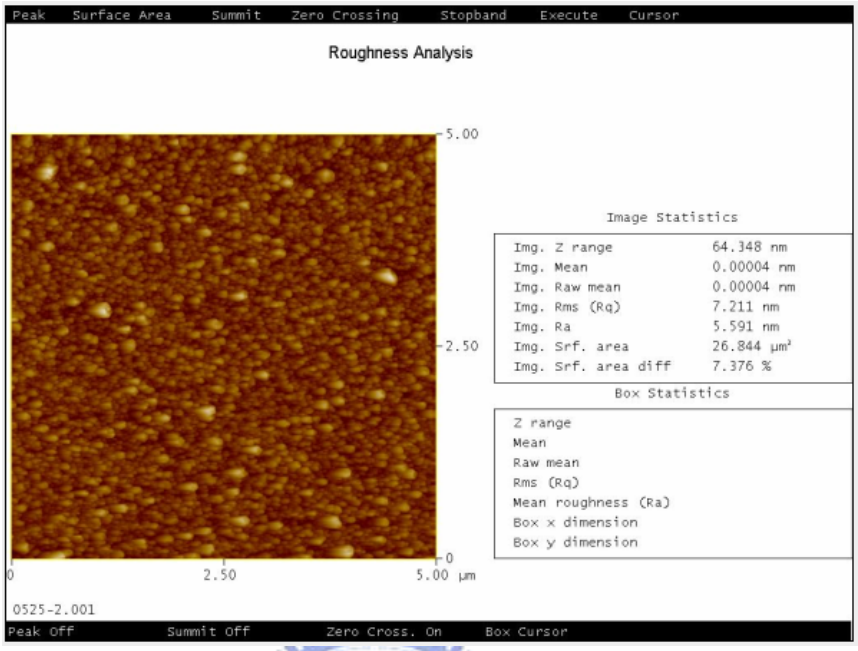

(c)

Figure 4-1 AFM images of iron film under different pre-treatment times

(a) only annealing (b) 5 min pre-treatment

(c) 10 min pre-treatment

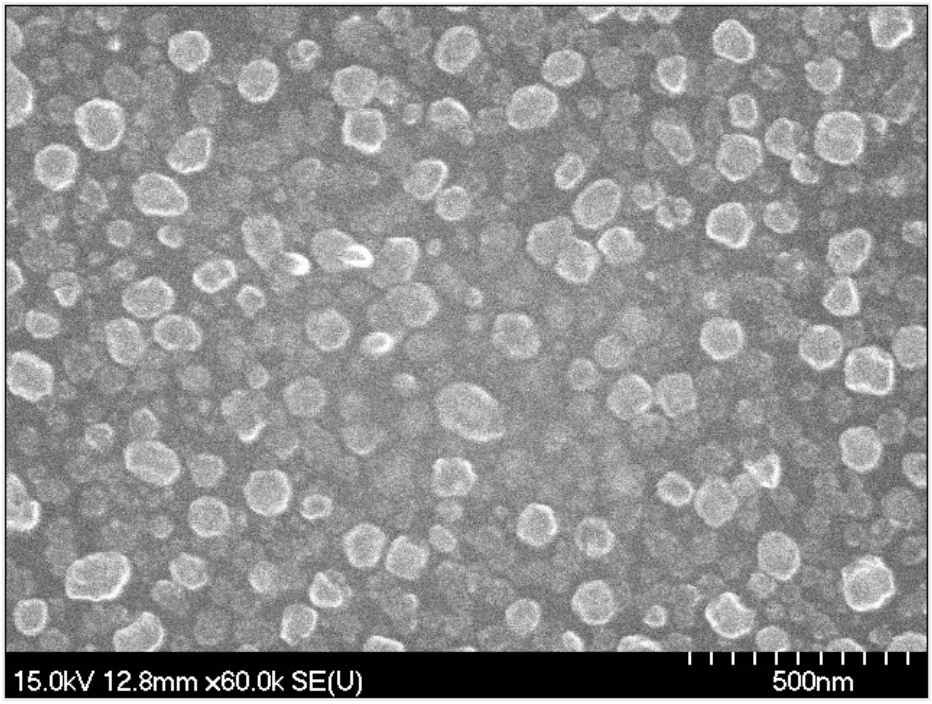

(a)

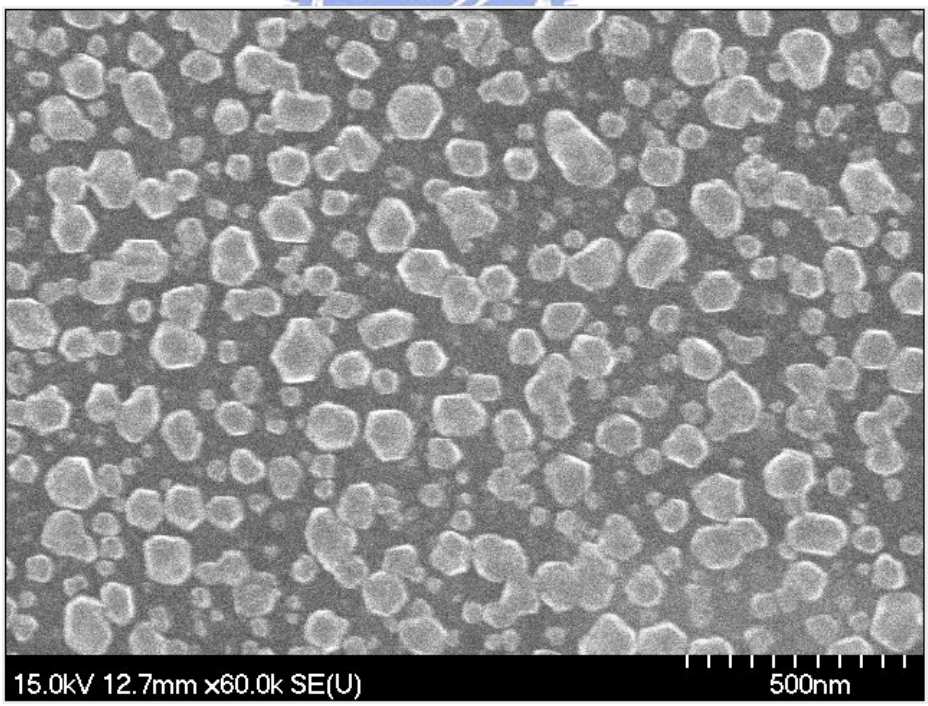

(b)

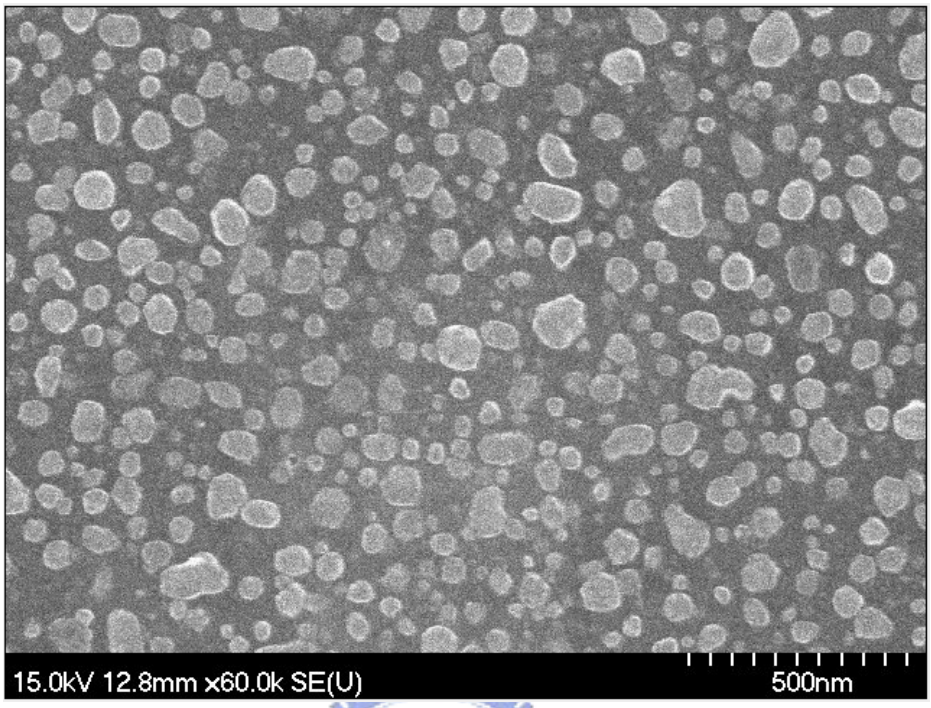

(c)

Figure4-2 SEM images of iron film under different pre-treatment times

(a) only annealing (b) 5 min pre-treatment

(c) 10 min pre-treatment